


ORIGINAL RESEARCH

Biosynthesis of silver nanoparticles using *Lawsonia inermis* and their biomedical application

Eman Alhomaidi¹ | Saade Abdalkareem Jasim² | Hawraz Ibrahim M. Amin^{3,4} |
Marcos Augusto Lima Nobre⁵ | Mehrdad Khatami⁶ | Abduladheem Turki Jalil⁷  |
Saja Hussain Dilfy^{8,9}

¹Department of Biology, College of Science, Princess Nourah bint Abdulrahman University, Riyadh, Saudi Arabia

²Al-Maarif University College, Medical Laboratory Techniques Department, Al-Anbar-Ramadi, Iraq

³Department of Chemistry, College of Science, Salahaddin University-Erbil, Erbil, Iraq

⁴Department of Medical Biochemical Analysis, Cihan University-Erbil, Erbil, Iraq

⁵São Paulo State University (Unesp), School of Technology and Sciences, Presidente Prudente, Sao Paulo, Brazil

⁶Antibacterial Materials R&D Centre, China Metal New Materials (Huzhou) Institute, Huzhou, Zhejiang, China

⁷Department of Medical Laboratories Techniques, Al-Mustaqbal University College, Babylon, Iraq

⁸Medical Laboratory Technology Department, College of Medical Technology, The Islamic University, Najaf, Iraq

⁹Department of Biology, College of Education for Pure Science, Wasit University, Iraq

Correspondence

Abduladheem Turki Jalil, Department of Medical Laboratories Techniques, Al-Mustaqbal University College, Babylon, 51001, Iraq.
Email: abedalazeem799@gmail.com

Funding information

Princess Nourah bint Abdulrahman University, Grant/Award Number: PNURSP2022R317; Princess Nourah bint Abdulrahman University, Riyadh, Saudi Arabia

Abstract

Developing biosynthesis of silver nanoparticles (Ag-NPs) using plant extract is an environmentally friendly method to reduce the use of harmful chemical substances. The green synthesis of Ag-NPs by *Lawsonia inermis* extract and its cellular toxicity and the antimicrobial effect was studied. The physical and chemical properties of synthesised Ag-NPs were investigated using UV-visible spectroscopy, infrared spectroscopy, X-ray diffraction (XRD), scanning, and transmission electron microscopy. The average size of Ag-NPs was 40 nm. The XRD result shows peaks at $2\theta = 38.07^\circ$, 44.26° , 64.43° , and 77.35° are related to the FCC structure of Ag-NPs. Cytotoxicity of synthesised nanoparticles was evaluated by MTT toxicity test on breast cancer MCF7 cell line. Observations showed that the effect of cytotoxicity of nanoparticles on the studied cell line depended on concentration and time. The obtained IC_{50} was considered for cells at a dose of 250 $\mu\text{g/ml}$. Growth and survival rates decreased exponentially with the dose. Antimicrobial properties of Ag-NPs synthesised with extract were investigated against *Escherichia coli*, *Salmonella typhimurium*, *Bacillus cereus*, and *Staphylococcus aureus* to calculate the minimum inhibitory concentration and the minimum bactericidal concentration of (MBC). The results showed that the synthesised Ag-NPs and the plant extract have antimicrobial properties. The lowest concentration of Ag-NPs that can inhibit the growth of bacterial strains was 25 $\mu\text{g/ml}$.

KEYWORDS

AgNPs, antibacterial activity, *Lawsonia inermis*, UV-visible spectroscopy, X-ray diffraction

This is an open access article under the terms of the Creative Commons Attribution-NoDerivs License, which permits use and distribution in any medium, provided the original work is properly cited and no modifications or adaptations are made.

© 2022 Antibacterial Materials R&D Centre, Metal New materials Institute. *IET Nanobiotechnology* published by John Wiley & Sons Ltd on behalf of The Institution of Engineering and Technology.

1 | INTRODUCTION

Nano comes from an ancient Greek word, and in the metric system, the term 'nanometre' means one-billionth of a metre [1]. Nano-sized particles are called nanoparticles [2]. Nanotechnology is an interdisciplinary knowledge of various disciplines [3, 4], including physics [5, 6], materials [7–9], engineering [10–12], mechanical engineering [13–16], agriculture [17], energy [18–20] and biology [21–25]. Recently, nanoparticles have been successfully used for sustained drug release [26], photo-catalytic [27–29], degradation [30–34], detection [35–39], treatment of infections [40], and in the food industry as potent anti-oxidant [41, 42], larvicidal [43], anti-fungal [44] and antibacterial agents [45, 46]. Various methods for producing nanoparticles are classified into three general methods: physical, chemical, and biological [47, 48]. Production is carried out by a simple chemical method, but there is a possibility that toxic substances resulting from the reaction will remain on the produced nanoparticles. There are standard chemical methods for preparing and manufacturing nanomaterials, such as sol-gel [49]. Due to the use of hazardous chemical substances, the nanoparticles resulting from these methods carry out reactions under particular conditions (temperature and pressure), which are expensive and time-consuming and create potential environmental risks. The physical method of nanoparticles has low toxicity, but it is most time consuming, dependent on expensive equipment, and has high energy consumption [50]. Due to these disadvantages and problems of using physical and chemical methods, the biological production method using plant extract is of interest today [48, 51, 52]. Plant extracts are considered to be the most pressing sources of biomolecules [53–56] such as proteins, nucleic acids [57], oils [58–61] and carbohydrates [62, 63]. Plant biomolecules have been identified to play an active role in the formation of nanostructures [64]. Biological methods are easy and cheap and have less toxicity [65] and production of toxic byproducts than common chemical and physical methods [66]. This method of producing nanoparticles is called the green method [67]. The energy consumption in this method is much less than chemical methods, and due to the compatibility with the environment, it is necessary to develop green methods [68]. New developments in science [69–75] and technology [76] have significant impact on human health [77–81] and life [82, 83].

Green methods [84] produced various silver [85], gold [86], copper [87], zinc [88], yttrium oxide [89], chromium (III) oxide [90], iron [91, 92], gallium nitride [93], boron nitride [94], aluminum nitride [95], calcium [96], zirconium/zirconium dioxide [97–99], palladium [100, 101], and tin oxide [102] nanoparticles. Gold and Ag-NPs have many applications in producing antimicrobial substances and diagnostic kits. Silver and gold have been used since ancient times because they have strong antibacterial [103], antifungal and antiviral properties [104]. Ag-NPs are helpful in different research fields such as medicine research [105] and nanoelectronics. Also, they can destroy cancer cells [106]. These particles can bind to cancer cells through a molecular coating and destroy the cancer cells.

Also, new technologies have recently been developed to treat infection [83, 107–111] and cancerous tumours [112–114].

Ag-NPs are a suitable option for preparing a new generation of anticancer and antimicrobial agents due to their intense biocidal activity and specific mechanism of action [115, 116]. Ag-NPs also disrupt biofilm formation. Although silver has been used as an antibacterial agent for centuries, recently, scientists have paid much attention to this element to solve the problem of drug resistance due to the improper use of antibiotics [117–119]. Studies show that by binding to the bacterial cell wall, Ag-NPs disrupt the cell wall's permeability and damage the cell. Ag-NPs also penetrate the cell and form a complex with thiol groups in the amino acid cysteine, thereby inactivating the vital enzymes of cell growth. Also, nanoparticles cause the formation of toxic free radicals such as superoxide, hydrogen peroxide, and hydroxyl ions and affect cellular respiration [120].

They were considering that the study on the toxicity of biogenic Ag-NPs produced by a green method using *Lawsonia inermis* has not been reported so far. Therefore, the present study aims to produce Ag-NPs by plant extract and investigate their antimicrobial and cytotoxic effects on Breast cancer cell lines.

2 | MATERIAL AND METHOD

2.1 | Synthesis of Ag-NPs

Lawsonia inermis leaves were collected from a local market in Kerman, Iran. To remove any dust contents from leaves, the surface was washed with water, then washed twice with sterile distilled water and dried at 25°C.

The method reported by Khatami et al. [121] was used for the green synthesis of Ag-NPs. Briefly, silver nitrate stock was prepared with a concentration of 500 mg in 50 ml of deionised water. Five grams of *L. inermis* dry leaf powder was added to 100 ml of deionised water and heated at 75°C for 15 min. After filtering through Whatman No. 40 filter paper, the filtered extract was used to synthesise Ag-NPs.

For the synthesis of Ag-NPs, leaf extract and AgNO₃ were mixed. In order to determine the optimal ratios, the extract and silver nitrate solution was used in ratios of 1:1, 2:1, and 3:1, respectively, and the optimal ratio at which the synthesis of Ag-NPs occurred was determined. In order to determine the optimal ratios, the visual colour change was the first visible sign of Ag-NPs synthesis with the naked eye. Concentrations in which no colour change was observed were determined as non-optimal ratios and were excluded from further study. Finally, the optimal concentration of the extract and AgNO₃ solution was used for the synthesis and determination of the properties of the synthesised Ag-NPs. The synthesis of Ag-NPs was investigated by UV-vis spectral analysis after observing the colour change of the reaction mixture to dark brown. Nanoparticles synthesised with plant extract were first centrifuged at 12,000 rpm for 10 min and settled. They have dissolved again in deionised water. Then, centrifugation was performed at

13,000 rpm to separate the synthesised nanoparticles. It was repeated two times between the operations. Then the synthesised Ag-NPs were dried and used to determine other physicochemical properties.

2.2 | Determination of physicochemical properties

To determine the size, structural properties, and morphology of Ag-NPs synthesised from plant extract, spectrophotometer devices (Biotek, US), X-ray diffraction (XRD) devices, field emission scanning electron microscope (FESEM), and transmission electron microscope (TEM) were analysed. The XRD pattern was used to determine the crystalline phases of synthesised Ag-NPs, measure the crystal constants of Ag-NPs and calculate the crystal size. To prepare the XRD pattern, a Philips X'pert Pro device made in the Netherlands was used with a Cu K α copper anode lamp source with a wavelength of $\lambda = 1.5406 \text{ \AA}$. To determine the size and dispersion distribution of Ag-NPs synthesised from plant extract, an LEO-912AB TEM with an applied voltage of 120 kV was used to emit electron beams [122]. The morphology of Ag-NPs synthesised from the extract was investigated by FESEM. To prepare the sample for imaging, the nanoparticle powder is covered with a skinny layer of gold to make the surface conductive so that it does not change the path of the returning electron beams. Also, the Ag-NP powder should be spread on a surface that is more conductive than aluminum. The FTIR spectroscopic test was performed to identify active groups and reducing groups of silver ions in the range of 500–3500 cm^{-1} [123, 124].

2.3 | Investigation of cytotoxicity

In the MTT method, the viability or non-viability of cells in the mitochondrial respiratory cycle was investigated. For this purpose, the MCF7 cell line was obtained from the Pasteur Institute of Iran and cultured in an RPMI1640 culture medium enriched with 10% FBS serum. Then, they were kept in a cell culture flask at 37°C in a humid atmosphere with a concentration of 5% CO₂. The cells were collected from the flask, and after adding the culture medium, the cell suspension was transferred to each well of the 96-well plate with a volume of 100 μl of the cell suspension and the amount of 10,000 cells. Then it was incubated under culture conditions. After 24 h, the culture medium was drained, and Ag-NPs with concentrations of 1–500 $\mu\text{g/ml}$ were added to each well. In the control group in this test, wells containing untreated cells were considered. After incubation, 10 μL of MTT dye (tetrazolium salt) with a concentration of 5 mg/ml were added to each well in the dark, and the incubation was done for 4 h. Then, 100 μl of Dimethyl Sulfoxide (DMSO) were added to each well. The optical absorbance of the samples was read with an ELISA device, and the results of the absorbance value were recorded at a wavelength of 570 nm. The results were calculated in terms of the percentage of living cells treated compared to untreated

from the following equation: $100 \times (\text{optical absorbance of untreated cells} / \text{optical absorbance of cells treated with nanoparticles}) = \% \text{ living cells}$.

2.4 | Cell viability percentage using cell proliferation kit

After the culture cells covered more than 85% of the culture flasks, they were re-suspended by trypsinisation. Cell viability was determined with trypan blue solution; after 24 h of incubation, the cells were exposed to different concentrations of Ag-NPs. They were incubated for 24 h. Cell viability was determined at the end of the period using a cell proliferation kit. The absorbance values of the cells in each well were checked at 450 nm. Cell viability percentage values were calculated.

2.5 | Investigating the antioxidant effect

Cell extracts were first prepared to investigate the effect of Ag-NPs on the activity of antioxidant enzymes in the tested cells. After cultivation and treatment, the cells were separated using EDTA trypsin. After centrifugation, they were washed twice with cold PBS. Then 300 μl of lysate buffer were added to the sediment of the cells, and after 20 min of centrifugation at 4°C With 10,000 RPM, the resulting supernatant was used to perform the test. The measurement of the total protein of the samples was done using the Bradford method. Also, the superoxide dismutase enzyme was measured based on the inhibition of nitroblue tetrazolium reduction by the enzyme

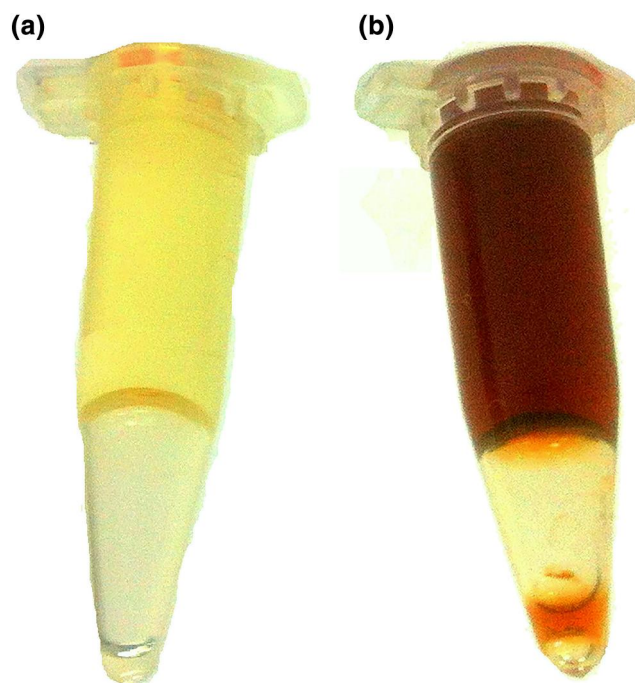


FIGURE 1 Colour change from pale yellow (plant extract) to dark brown (Ag-NPs)

present in the sample. The measurement of catalase was also based on the reduction of hydrogen peroxide per unit of time due to the enzyme activity in the sample.

2.6 | Investigation of antimicrobial effect

Bacterial pathogens of *Escherichia coli*, *Salmonella typhimurium*, *Bacillus cereus*, and *Staphylococcus aureus* were obtained

from the Centre of Biological and Genetic Resources of Iran. The antimicrobial activity of the Ag-NPs was measured by measuring the halo of non-growth and diffusion method from the well on the agar surface. In this method, after preparing a microbial suspension with turbidity equal to half McFarland ($\text{CFU/ml } 10^8$), cultivation was done using a sterile glass rod on the surface of the Mueller Hinton agar culture medium. After drying the surface of the culture medium plates, with the help of a sterile Pasteur pipette, three wells with a diameter of 5 mm

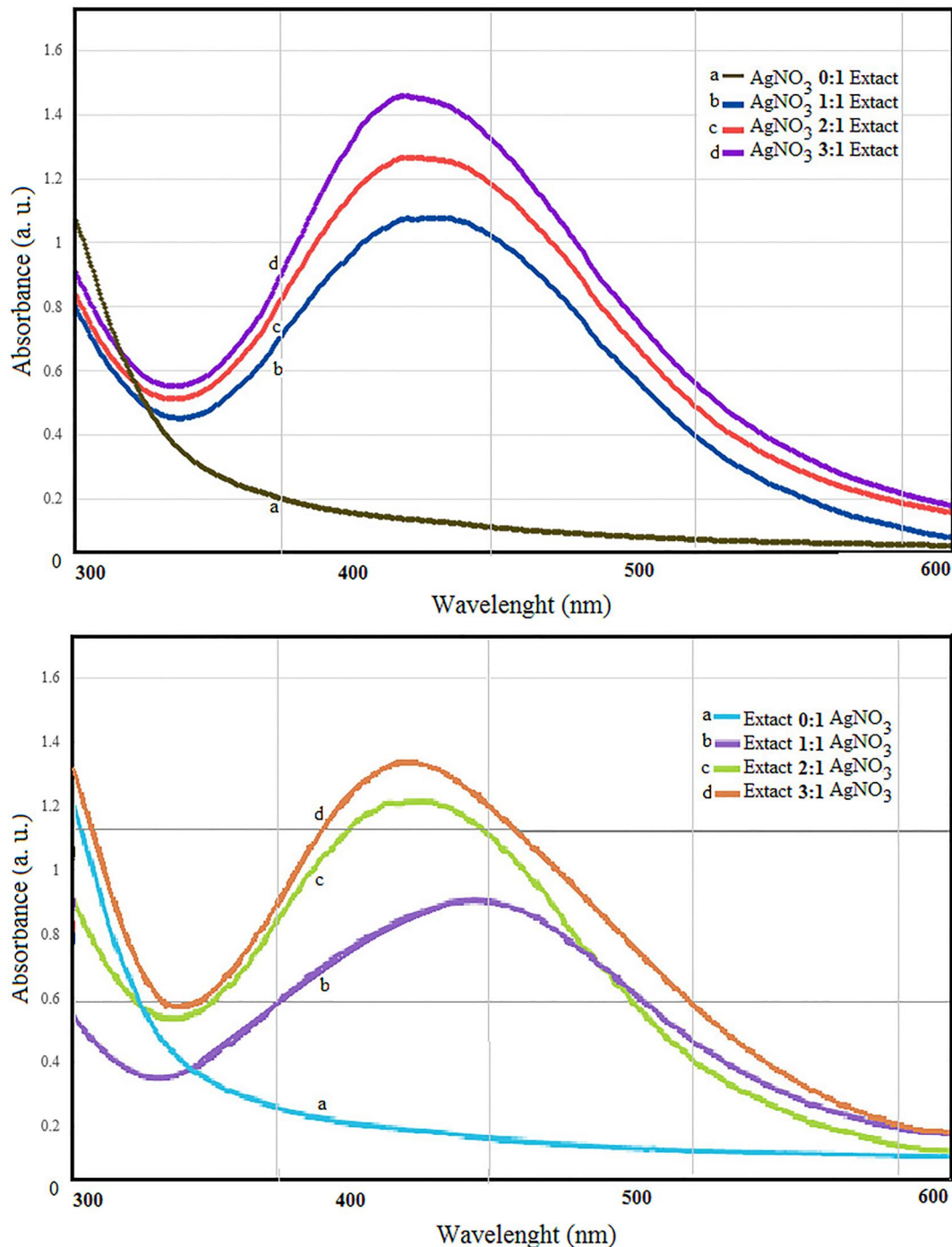


FIGURE 2 UV-visible spectrum of Ag-NPs synthesised with different ratios (0:1, 1:1, 2:1, and 3:1) of extract and silver nitrate solution

were created at a suitable distance from each other. Then, 50 ml of the Ag-NPs were poured into the created wells after being dispersed in sterile deionised water using an ultrasonic bath. The plates were incubated for 24 h at 37°C. Double distilled water on a blank disk was used as a negative control. Finally, the sensitivity of bacteria was measured by measuring the diameter of the non-growth halo with the help of callipers. This experiment was repeated three times for each bacterium, and the arithmetic mean of the area diameter (mm) was reported.

2.7 | Statistical analysis

Data were recorded as mean with standard deviation. One-way analysis of variance (ANOVA) was used to identify significant differences between the tested groups. All data analyses were evaluated based on significance at the 0.05 level.

3 | RESULTS

Ag-NPs were synthesised by aqueous extract. The colour change from pale yellow to dark brown indicates the production of Ag-NPs (Figure 1).

The results of the spectrophotometric analysis with ultraviolet light in the control sample (extract alone) and after the synthesis of Ag-NPs are shown in Figure 2. The increase in absorbance in the range of 450–500 nm indicates the synthesis of Ag-NPs. The UV-Vis spectrum shows a surface plasmon resonance (SPR) of Ag-NPs at about 420 nm [125, 126].

The results of FTIR spectroscopic analysis before and after the reaction with silver nitrate are shown in Figure 3. The comparison of two spectroscopic graphs shows the aqueous extract's biological power in reducing silver ions. There are

peaks related to vibrations at wavelengths of 599, 674, 1151, 2357, and 3446, which are, respectively, related to alkyl, alkene, carbonyl (CO), CO₂, and hydroxyl (OH) groups [127, 128].

Figure 4 shows electron microscope images (TEM) of Ag-NPs synthesised with plant extract. As it is clear from the images, the Ag-NPs in the image have a spherical shape and have a proper distribution, and around the nanoparticles, a bright background can be seen, which is related to the extract because the density of the extract is different from the light passing through the density. Ag-NPs are few, so Ag-NPs are darker in the image, and the solvent is brighter. According to the TEM image, the size of nanoparticles has a diameter ranging from 20 to 70 nm; with a normal distribution, the average diameter is around 40 nm.

Figure 5a shows FESEM images of Ag-NPs synthesised with plant extract. The FESEM image shows the silver particles' nm dimensions and an almost spherical shape in all magnifications. Determining the size of Ag-NPs through FESEM is not accurate because the resolving power of FESEM is lower than that of TEM, so TEM analysis was used to report the average size. According to FESEM images, the cumulative size of nanoparticles is below 100 nm. In the EDX analysis, the peak related to silver metal was seen, indicating that the Ag-NPs observed in the SEM images are made of silver (Figure 5b). Observing the optical absorption band at 3 Kev indicates the presence of silver metal nanoparticles. Of course, the presence of peaks of elements C and O in the EDX spectrum is related to the residues caused by the substances in the supernatant of the extract, such as enzyme or protein residues.

Figure 6 shows the XRD pattern of plant extract alone (Figure 6a) and Ag-NPs (Figure 6b). As can be seen, the peaks at $2\theta = 38.07^\circ, 44.26^\circ, 64.43^\circ,$ and 77.35° corresponding to (111), (200), (220), and (311) are related to the FCC structure of Ag-NPs, which is in perfect agreement with the standard XRD pattern of silver. The crystal size of Ag-NPs is obtained

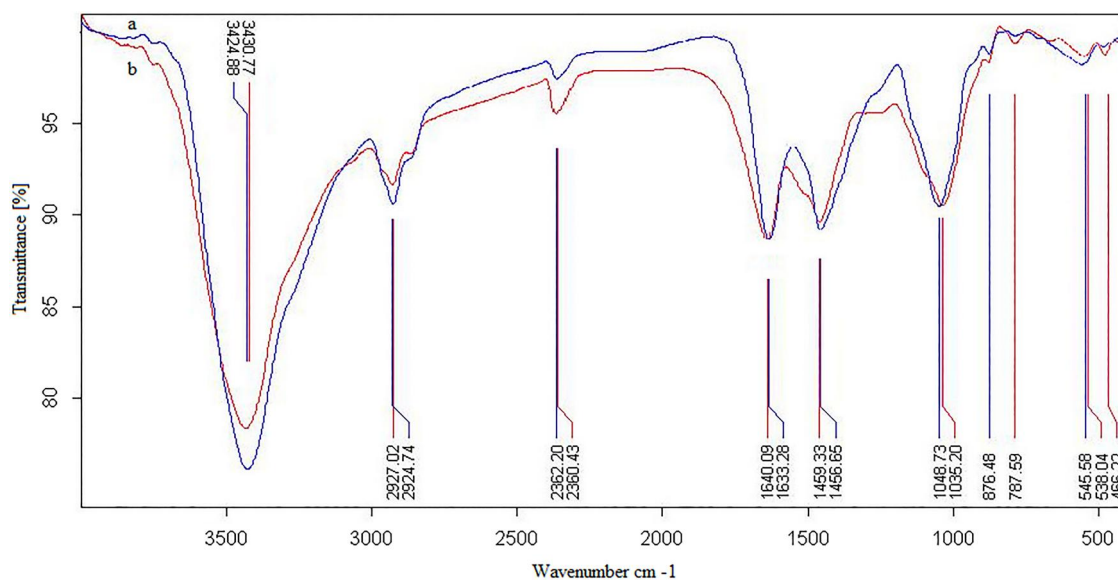


FIGURE 3 FTIR spectrum before (a) and after (b) the synthesis of Ag-NPs

from Scherrer equation: $L = K\lambda/\beta \cdot \cos\theta$. In this equation, $k = 0.9$ is the shape factor and λ is the wavelength of the X-ray and is equal to 1.5406 \AA . β is the full width at half the maximum of the diffraction peak, and θ is the angle corresponding to the diffraction peak. From the calculation of Scherrer's relation, the crystal size of nanoparticles is 40 nm , which is consistent with TEM images.

MTT test was performed to investigate the effect of Ag-NPs on cell viability for 24 h and with concentrations of $1\text{--}500 \text{ }\mu\text{g/ml}$. The statistical results showed that the viability of the cells after exposure to these doses of Ag-NPs decreased significantly compared to the control sample (Figure 7). The obtained IC_{50} was considered for cells at a dose of $250 \text{ }\mu\text{g/ml}$. Growth and survival rates decreased exponentially with the dose.

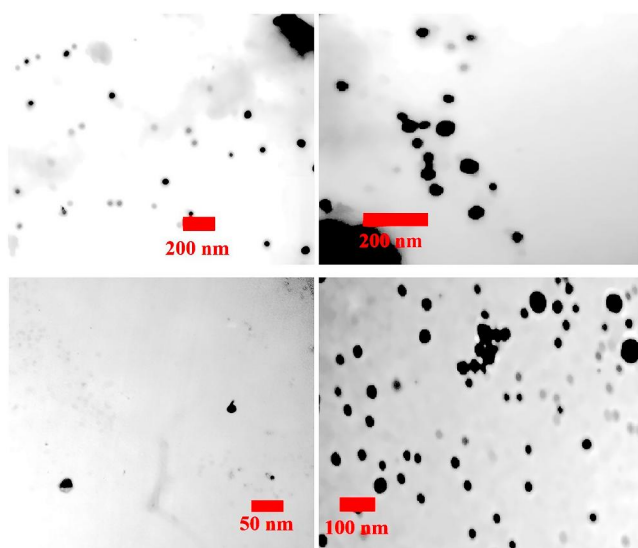


FIGURE 4 TEM images of synthesised Ag-NPs

In cell treatment groups, the IC_{50} concentration of Ag-NPs overtime on days 1%, 2% and 5% of cell survival decreased. The trypan blue staining method was also used to confirm the results of the MTT assay. Cells after treatment with IC_{50} concentration of Ag-NPs treatment on days 1, 2 and 5 with trypan blue dye were counted using a neobar slide. This method confirmed the results of the MTT assay. On the fifth day after the treatment, all the cells of the treatment group were separated from the bottom of the well and placed in cell count under the neobar slide was not seen.

After treatment with IC_{50} concentration of Ag-NPs, cancer cells were observed and examined with a microscope. Compared to the control group, changes were observed in the cell morphology of the treatment groups, including cell

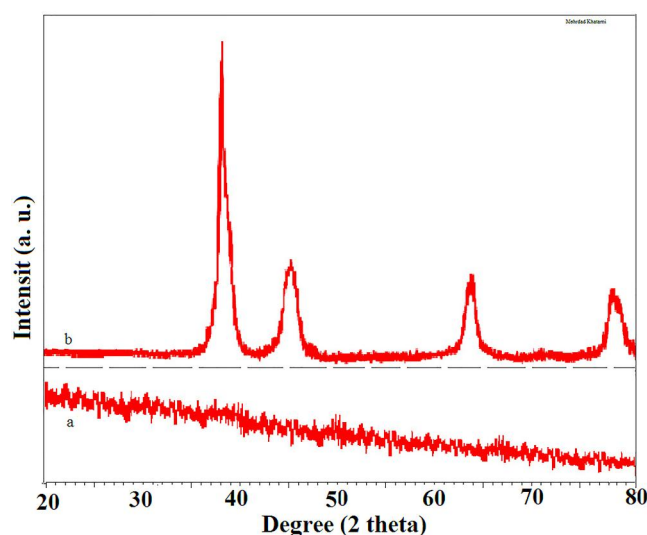


FIGURE 6 XRD pattern of plant extract (a) and resulting synthesised Ag-NPs (b)

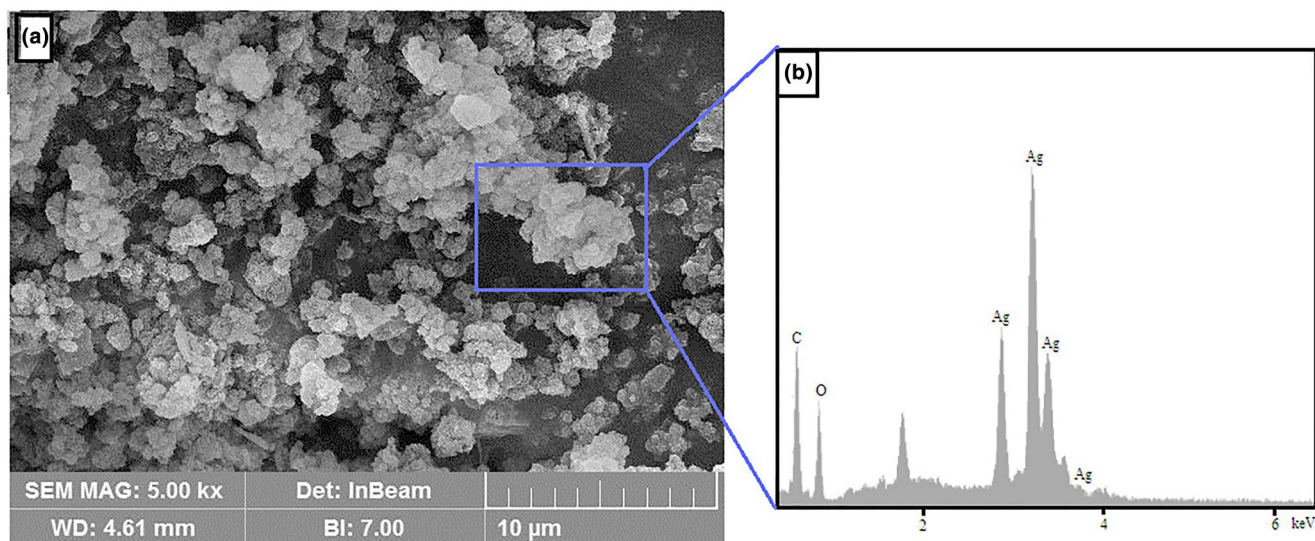


FIGURE 5 FESEM image (a) and EDX spectrum (b) of resulting green synthesised Ag-NPs

spheroidisation and shrivelling. Over time, these changes were observed in a more significant number of treatment cells so that after 2 days, the cells of the treatment group were suspended and dead. In order to more closely examine the morphological changes after the treatment of the cells, they were stained with Giemsa dye and observed by an optical microscope. The morphology of the cells in the control sample was utterly ordinary, so the cells were with healthy membranes and some were seen dividing. However, the treated cells showed changes such as a reduction in cell volume, cell granulation, chromatin condensation inside the nucleus, and the production of apoptotic bodies.

To determine the type of cell death induced by nanoparticles on the cell line, the acridine orange/ethidium bromide staining method was used. In this staining, living cells are seen in green, while cells in the apoptosis stage are seen in orange. In the groups treated with Ag-NPs, the number of cells with orange colour increased significantly compared to the control group.

The Bradford method was used to measure the protein concentration in all samples (treatment and control), and its standard diagram was first drawn. Then, using the standard graph and its line equation, the protein concentration was measured. Protein concentration was measured to express the amount of enzyme activity in milligrams of protein. After calculating the amount of superoxide dismutase and catalase enzymes in the control group, the treated group with IC_{50} concentration of Ag-NPs and statistical analysis, a diagram was drawn. The results showed that the activity of the superoxide dismutase enzyme in the Ag-NP treatment group was significantly increased compared to the control ($P < 0.001$). The results showed that the catalase enzyme activity increased significantly in the Ag-NP treatment group compared to the control group ($P < 0.05$).

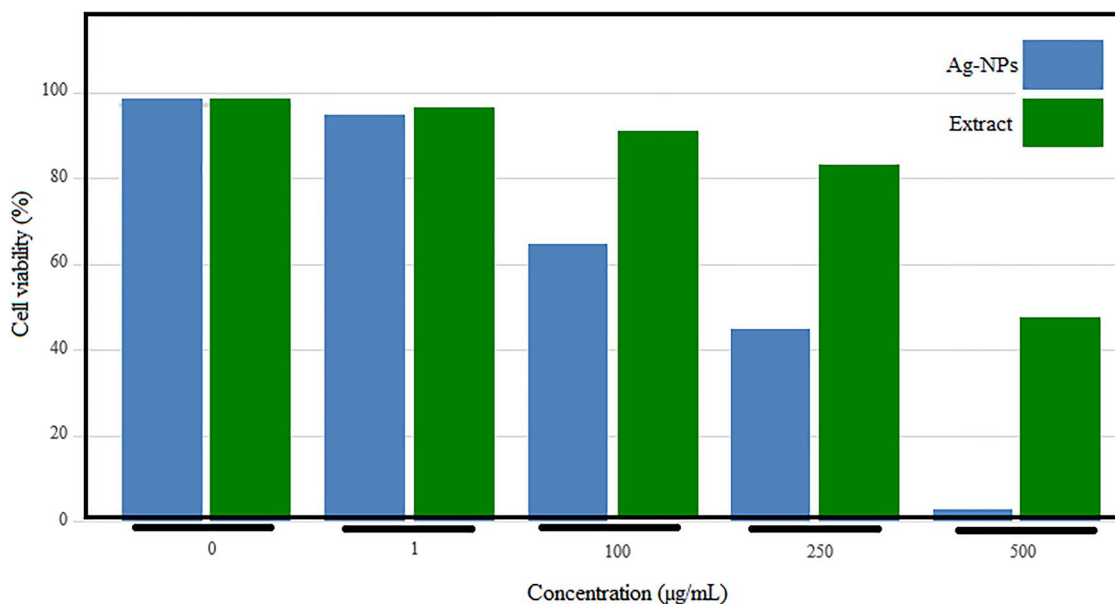


FIGURE 7 The cell viability of MCF-7 cells treated with Ag-NPs

In short, the most common mechanism for the antibacterial effect of Ag-NPs is that Ag-NPs release ionic silver and deactivate the thiol groups in the enzymes, which cause the inactivation of bacterial enzymes. The released silver ions inhibit bacterial DNA replication, damage the cell cytoplasm, decrease the level of adenosine triphosphate (ATP) and ultimately lead to the death of the bacterial cell. Increasing the ratio of the surface area to the volume of nanoparticles increases the level of attachment of nanoparticles to bacterial cells and increases the release of silver ions to bacteria, thus improving the antibacterial effect of silver [129].

DPPH radical was used to evaluate natural antioxidants' free radical scavenging activity [130]. The results showed that Ag-NPs synthesised with leaf extract showed free radical inhibition activity. The antioxidant activity or, in other words, the free radical scavenging activity of Ag-NPs synthesised by the leaf extract increased dose-dependent (Figure 8).

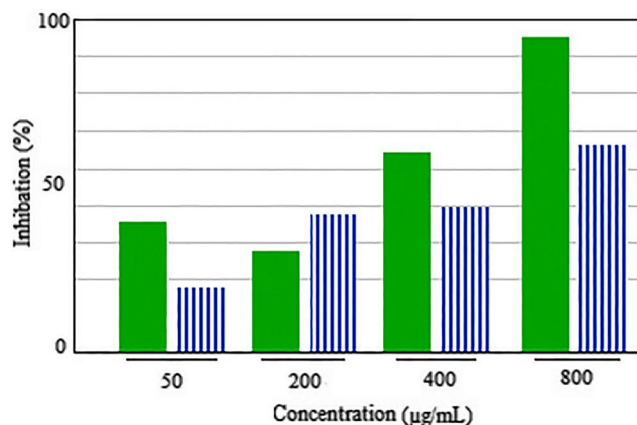


FIGURE 8 DPPH radical Ag-NPs

4 | CONCLUSION

In this research, the possibility of producing Ag-NPs by *L. inermis* extract and its antimicrobial and anticancer effects were studied. Based on the results, Ag-NPs produced by aqueous extract had a size of less than 100 and showed effective antimicrobial and anticancer activity. These particles caused the non-growth of tested bacteria, and gram-negative bacteria are more sensitive than gram-positive bacteria. The synthesis of Ag-NPs can be produced on an industrial scale without needing expensive raw materials. Considering the antimicrobial property of these particles on the tested strains, they can be used as an effective disinfectant for sterilising the hospital environment and disinfecting hospital waste. Ag-NPs reduce the survival of cancer cells in a dose-dependent manner. Ag-NPs synthesised from *L. inermis* extract can be used in breast cancer treatment.

ACKNOWLEDGEMENT

This work was funded by Princess Nourah Bint Abdulrahman University Researchers Supporting Project number (PNURSP2022R317), Princess Nourah bint Abdulrahman University, Riyadh, Saudi Arabia.

CONFLICT OF INTEREST

The authors declare that they have no conflict of interest.

DATA AVAILABILITY STATEMENT

The data that support the findings of this study are available from the corresponding author upon reasonable request.

ORCID

Abdulbheem Turki Jalil  <https://orcid.org/0000-0001-8403-7465>

REFERENCES

- Jasim, S.A., et al.: Green synthesis of spinel copper ferrite (CuFe₂O₄) nanoparticles and their toxicity. *Nanotechnol. Rev.* 11(1), 2483–2492 (2022). <https://doi.org/10.1515/ntrev-2022-0143>
- Moghadam, N.C.Z., et al.: Nickel oxide nanoparticles synthesis using plant extract and evaluation of their antibacterial effects on *Streptococcus mutans*. *Bioproc. Biosyst. Eng.* 45(7), 1201–1210 (2022). <https://doi.org/10.1007/s00449-022-02736-6>
- Zhang, Y., et al.: Nano-enhanced biolubricant in sustainable manufacturing: from processability to mechanisms. *Friction.* 10(6), 803–841 (2022). <https://doi.org/10.1007/s40544-021-0536-y>
- Jasim, S.A., et al.: MXene/metal and polymer nanocomposites: preparation, properties, and applications. *J. Alloys Compd.* 917, 165404 (2022). <https://doi.org/10.1016/j.jallcom.2022.165404>
- Gao, T., et al.: Surface morphology assessment of CFRP transverse grinding using CNT nanofluid minimum quantity lubrication. *J. Clean. Prod.* 277, 123328 (2020). <https://doi.org/10.1016/j.jclepro.2020.123328>
- Jia, D., et al.: Experimental verification of nanoparticle jet minimum quantity lubrication effectiveness in grinding. *J. Nanoparticle Res.* 16(12), 1–15 (2014). <https://doi.org/10.1007/s11051-014-2758-7>
- Min, Y., et al.: Predictive model for minimum chip thickness and size effect in single diamond grain grinding of zirconia ceramics under different lubricating conditions. *Ceram. Int.* 45(12), 14908–14920 (2019). <https://doi.org/10.1016/j.ceramint.2019.04.226>
- Duan, Z., et al.: Milling force model for aviation aluminum alloy: academic insight and perspective analysis. *Chin. J. Mech. Eng.* 34(1), 1–35 (2021). <https://doi.org/10.1186/s10033-021-00536-9>
- Xin, C., et al.: Minimum quantity lubrication machining of aeronautical materials using carbon group nanolubricant: from mechanisms to application. *Chin. J. Aeronaut.* (2021). <https://doi.org/10.1016/j.cja.2021.08.011>
- Gao, T., et al.: Dispersing mechanism and tribological performance of vegetable oil-based CNT nanofluids with different surfactants. *Tribol. Int.* 131, 51–63 (2019). <https://doi.org/10.1016/j.triboint.2018.10.025>
- Gao, T., et al.: Carbon fiber reinforced polymer in drilling: from damage mechanisms to suppression. *Compos. Struct.* 286, 115232 (2022). <https://doi.org/10.1016/j.compstruct.2022.115232>
- Salahdin, O.D., et al.: Current challenges in seismic drilling operations: a new perspective for petroleum industries. *Asian J. Water Environ. Pollut.* 19(3), 69–74 (2022). <https://doi.org/10.3233/ajw220041>
- Zhang, Y., et al.: Experimental evaluation of the lubrication performance of MoS₂/CNT nanofluid for minimal quantity lubrication in Ni-based alloy grinding. *Int. J. Mach. Tool Manufact.* 99, 19–33 (2015). <https://doi.org/10.1016/j.ijmactools.2015.09.003>
- Yang, M., et al.: Predictive model of convective heat transfer coefficient in bone micro-grinding using nanofluid aerosol cooling. *Int. Commun. Heat Mass Tran.* 125, 105317 (2021). <https://doi.org/10.1016/j.icheatmasstransfer.2021.105317>
- Gao, T., et al.: Mechanics analysis and predictive force models for the single-diamond grain grinding of carbon fiber reinforced polymers using CNT nano-lubricant. *J. Mater. Process. Technol.* 290, 116976 (2021). <https://doi.org/10.1016/j.jmatprotec.2020.116976>
- Xia, J., Majidi, A., Toghraie, D.: Molecular dynamics simulation of friction process in atomic structures with spherical nanoparticles. *Solid State Commun.* 346, 114717 (2022). <https://doi.org/10.1016/j.ssc.2022.114717>
- Zhang, Y., et al.: Experimental evaluation of MoS₂ nanoparticles in jet MQL grinding with different types of vegetable oil as base oil. *J. Clean. Prod.* 87, 930–940 (2015). <https://doi.org/10.1016/j.jclepro.2014.10.027>
- Salahdin, O.D., et al.: Oxygen reduction reaction on metal-doped nanotubes and nanocages for fuel cells. *Ionics.* 28(7), 3409–3419 (2022). <https://doi.org/10.1007/s11581-022-04564-w>
- Al-Nayili, A., et al.: Formic acid dehydrogenation using noble-metal nanoheterogeneous catalysts: towards sustainable hydrogen-based energy. *Catalysts.* 12(3), 324 (2022). <https://doi.org/10.3390/catal12030324>
- Sivaraman, R., et al.: Evaluating the potential of graphene-like boron nitride as a promising cathode for Mg-ion batteries. *J. Electroanal. Chem.* 917, 116413 (2022). <https://doi.org/10.1016/j.jelechem.2022.116413>
- Liu, M., et al.: Cryogenic minimum quantity lubrication machining: from mechanism to application. *Front. Mech. Eng.* 16(4), 649–697 (2021). <https://doi.org/10.1007/s11465-021-0654-2>
- Gao, T., et al.: Grindability of carbon fiber reinforced polymer using CNT biological lubricant. *Sci. Rep.* 11(1), 1–14 (2021). <https://doi.org/10.1038/s41598-021-02071-y>
- Alshehri, F., Al-Enazi, N.M., Ameen, F.: Vermicomposting Amended with Microalgal Biomass and Biochar Produce Phytopathogen-Resistant Seedbeds for Vegetables. *Biomass Conversion and Biorefinery* (2021)
- Kadri, S.U.T., et al.: Transcriptome-wide identification and computational insights into protein modeling and docking of CAMTA transcription factors in *Eleusine coracana* L. (finger millet). *Int. J. Biol. Macromol.* 206, 768–776 (2022). <https://doi.org/10.1016/j.ijbiomac.2022.03.073>
- Arkaban, H., et al.: Polyacrylic acid nanoplateforms: antimicrobial, tissue engineering, and cancer theranostic applications. *Polymers.* 14(6), 1259 (2022). <https://doi.org/10.3390/polym14061259>
- Singh, S.I., et al.: Vermiremediation of Allopathic Pharmaceutical Industry Sludge Amended with Cattle Dung Employing *Eisenia fetida*. *Environmental Research.* 113766 (2022)
- Indhira, D., et al.: Biomimetic facile synthesis of zinc oxide and copper oxide nanoparticles from *Elaeagnus indica* for enhanced photocatalytic

- activity. *Environ. Res.* 212, 113323 (2022). <https://doi.org/10.1016/j.envres.2022.113323>
28. Ameen, F., Dawoud, T., AlNadhari, S.: Ecofriendly and low-cost synthesis of ZnO nanoparticles from *Acremonium potronii* for the photocatalytic degradation of azo dyes. *Environ. Res.* 202, 111700 (2021). <https://doi.org/10.1016/j.envres.2021.111700>
 29. Megarajan, S., et al.: Synthesis of N-myristoyltaurine stabilized gold and silver nanoparticles: assessment of their catalytic activity, antimicrobial effectiveness and toxicity in zebrafish. *Environ. Res.* 212, 113159 (2022). <https://doi.org/10.1016/j.envres.2022.113159>
 30. Kandasamy, S., et al.: Laccase production from *Bacillus aestuarii* KSK using *Borassus flabellifer* empty fruit bunch waste as substrate and assess their malachite green dye degradation. *J. Appl. Microbiol.* (2022)
 31. Ameen, F., Al-Homaidan, A.A.: Improving the efficiency of vermicomposting of polluted organic food wastes by adding biochar and mangrove fungi. *Chemosphere.* 286, 131945 (2022). <https://doi.org/10.1016/j.chemosphere.2021.131945>
 32. Aljumaily, M.M., et al.: Modification of poly (vinylidene fluoride-co-hexafluoropropylene) membranes with DES-functionalized carbon nanospheres for removal of methyl orange by membrane distillation. *Water.* 14(9), 1396 (2022). <https://doi.org/10.3390/w14091396>
 33. Hachem, K., et al.: Adsorption of Pb (II) and Cd (II) by magnetic chitosan-salicylaldehyde Schiff base: synthesis, characterization, thermal study and antibacterial activity. *J. Chin. Chem. Soc.* 69(3), 512–521 (2022). <https://doi.org/10.1002/jccs.202100507>
 34. Anzum, R., et al.: A review on separation and detection of copper, cadmium, and chromium in food based on cloud point extraction technology. *Food Sci. Technol.*, 42 (2022). <https://doi.org/10.1590/fst.80721>
 35. Ngafwan, N., et al.: Study on novel fluorescent carbon nanomaterials in food analysis. *Food Sci. Technol.*, 42 (2021). <https://doi.org/10.1590/fst.37821>
 36. Jalil, A.T., et al.: High-sensitivity biosensor based on glass resonance PhC cavities for detection of blood component and glucose concentration in human urine. *Coatings.* 11(12), 1555 (2021). <https://doi.org/10.3390/coatings11121555>
 37. Chupradit, S., et al.: Ultra-sensitive biosensor with simultaneous detection (of cancer and diabetes) and analysis of deformation effects on dielectric rods in optical microstructure. *Coatings.* 11(12), 1564 (2021). <https://doi.org/10.3390/coatings11121564>
 38. Yumashev, A.V., et al.: Optical-based biosensor for detection of oncomarker CA 125, recent progress and current status. *Anal. Biochem.*, 114750 (2022). <https://doi.org/10.1016/j.ab.2022.114750>
 39. Chupradit, S., et al.: Various types of electrochemical biosensors for leukemia detection and therapeutic approaches. *Anal. Biochem.* 654, 114736 (2022). <https://doi.org/10.1016/j.ab.2022.114736>
 40. Fitriyah, A., et al.: Exposure to ambient air pollution and osteoarthritis; an animal study. *Chemosphere.* 301, 134698 (2022). <https://doi.org/10.1016/j.chemosphere.2022.134698>
 41. Ameen, F., et al.: Anti-oxidant, Anti-fungal and Cytotoxic Effects of Silver Nanoparticles Synthesized Using Marine Fungus *Cladosporium Halotolerans*, pp. 1–9. *Applied Nanoscience* (2021)
 42. Jumintono, J., et al.: Effect of cystamine on sperm and antioxidant parameters of ram semen stored at 4° C for 50 hours. *Arc Razi Ins.* 76(4), 115 (2021)
 43. Sonbol, H., et al.: Bioinspired Synthesis of CuO Nanoparticles Using *Cylindrospermum Stagnale* for Antibacterial, Anticancer and Larvicidal Applications, pp. 1–11. *Applied Nanoscience* (2021)
 44. Almansob, A., Bahkali, A.H., Ameen, F.: Efficacy of gold nanoparticles against drug-resistant nosocomial fungal pathogens and their extracellular enzymes: resistance profiling towards established antifungal agents. *Nanomaterials.* 12(5), 814 (2022). <https://doi.org/10.3390/nano12050814>
 45. Ameen, F., et al.: Antioxidant, Antibacterial and Anticancer Efficacy of *Alternaria Chlamyospora*-Mediated Gold Nanoparticles. *Applied Nanoscience* (2022)
 46. Bala Subramanian, S., et al.: Phytolectin-cationic lipid complex revive ciprofloxacin efficacy against multi-drug resistant uropathogenic *Escherichia coli*. *Colloids Surf. A Physicochem. Eng. Asp.* 647, 128970 (2022). <https://doi.org/10.1016/j.colsurfa.2022.128970>
 47. Ameen, F.: Optimization of the synthesis of fungus-mediated Bi-metallic Ag-Cu nanoparticles. *Appl. Sci.* 12(3), 1384 (2022). <https://doi.org/10.3390/app12031384>
 48. AlNadhari, S., et al.: A review on biogenic synthesis of metal nanoparticles using marine algae and its applications. *Environ. Res.* 194, 110672 (2021). <https://doi.org/10.1016/j.envres.2020.110672>
 49. Bokov, D., et al.: Nanomaterial by sol-gel method: synthesis and application. *Adv. Mater. Sci. Eng.*, 2021–21 (2021). <https://doi.org/10.1155/2021/5102014>
 50. Chen, F., et al.: Mitigation of lead toxicity in *Vigna radiata* genotypes by silver nanoparticles. *Environ. Pollut.* 308, 119606 (2022). <https://doi.org/10.1016/j.envpol.2022.119606>
 51. Mohanta, Y.K., et al.: Bio-inspired synthesis of silver nanoparticles from leaf extracts of *Cleistanthus collinus* (Roxb.): its potential antibacterial and anticancer activities. *IET Nanobiotechnol.* 12(3), 343–348 (2018). <https://doi.org/10.1049/iet-nbt.2017.0203>
 52. Ameen, F., et al.: Soil bacteria *Cupriavidus* sp. mediates the extracellular synthesis of antibacterial silver nanoparticles. *J. Mol. Struct.* 1202, 127233 (2020). <https://doi.org/10.1016/j.molstruc.2019.127233>
 53. Li, S., et al.: Prediction of oral hepatotoxic dose of natural products derived from traditional Chinese medicines based on SVM classifier and PBPK modeling. *Arch. Toxicol.* 95(5), 1683–1701 (2021). <https://doi.org/10.1007/s00204-021-03023-1>
 54. Adetomiwa, K., et al.: Sensitivity analysis and future farm size projection of bio-fortified cassava production in oyo state, nigeria. *Malaysian J Sus Agri.* 5(2), 61–66 (2020). <https://doi.org/10.26480/mjsa.02.2021.61.66>
 55. Gunawan, W., et al.: Effect of Tomato Consumption on Inflammatory Markers in Health and Disease Status: A Systematic Review and Meta-Analysis of Clinical Trials. *Clinical Nutrition ESPEN* (2022)
 56. Ghaffar, S., et al.: What is the influence of grape products on liver enzymes? A systematic review and meta-analysis of randomized controlled trials. *Compl. Ther. Med.* 69, 102845 (2022). <https://doi.org/10.1016/j.ctim.2022.102845>
 57. Zou, Q., et al.: Gene2vec: gene subsequence embedding for prediction of mammalian N6-methyladenosine sites from mRNA. *RNA* 25(2), 205–218 (2019). <https://doi.org/10.1261/rna.069112.118>
 58. Lai, W.-F., Tang, R., Wong, W.-T.: Ionically crosslinked complex gels loaded with oleic acid-containing vesicles for transdermal drug delivery. *Pharmaceutics.* 12(8), 725 (2020). <https://doi.org/10.3390/pharmaceutics12080725>
 59. Guo, S., et al.: Experimental evaluation of the lubrication performance of mixtures of castor oil with other vegetable oils in MQL grinding of nickel-based alloy. *J. Clean. Prod.* 140, 1060–1076 (2017). <https://doi.org/10.1016/j.jclepro.2016.10.073>
 60. Wang, Y., et al.: Processing characteristics of vegetable oil-based nanofluid MQL for grinding different workpiece materials. *Int J Precision Eng Manufac Green Techn.* 5(2), 327–339 (2018). <https://doi.org/10.1007/s40684-018-0035-4>
 61. Hussein, H.K., et al.: Association of cord blood asprosin concentration with atherogenic lipid profile and anthropometric indices. *Diabetol. Metab. Syndrome.* 14(1), 1–6 (2022). <https://doi.org/10.1186/s13098-022-00844-7>
 62. Cheng, M., et al.: Effect of dual-modified cassava starches on intelligent packaging films containing red cabbage extracts. *Food Hydrocolloids.* 124, 107225 (2022). <https://doi.org/10.1016/j.foodhyd.2021.107225>
 63. Lai, W.-F., et al.: A self-indicating cellulose-based gel with tunable performance for bioactive agent delivery. *J. Drug Deliv. Sci. Technol.* 63, 102428 (2021). <https://doi.org/10.1016/j.jddst.2021.102428>
 64. Cao, Y., et al.: Ceramic magnetic ferrite nanoribbons: eco-friendly synthesis and their antifungal and parasiticidal activity. *Ceram. Int.* 48(3), 3448–3454 (2021). <https://doi.org/10.1016/j.ceramint.2021.10.121>
 65. Zhang, J., et al.: Experimental assessment of an environmentally friendly grinding process using nanofluid minimum quantity lubrication with cryogenic air. *J. Clean. Prod.* 193, 236–248 (2018). <https://doi.org/10.1016/j.jclepro.2018.05.009>

66. Nordin, N.F.H., et al.: Pcb biodegradation using bacteria isolated from landfill leachate. *Science*. 1(2), 07–10 (2017). <https://doi.org/10.26480/gws.02.2017.07.10>
67. Nazari-pour, E., et al.: Ferromagnetic nickel (II) oxide (NiO) nanoparticles: biosynthesis, characterization and their antibacterial activities, pp. 1–8. *Rendiconti Lincei Scienze Fisiche e Naturali* (2022)
68. Akbarizadeh, M.R., Sarani, M., Darjani, S.: Study of antibacterial performance of biosynthesized pure and Ag-doped ZnO nanoparticles. *Rendiconti Lincei Scienze Fisiche e Naturali* (2022)
69. Vakili-Samiani, S., et al.: Targeting Wee1 kinase as a therapeutic approach in hematological malignancies. *DNA Repair* 107, 103203 (2021). <https://doi.org/10.1016/j.dnarep.2021.103203>
70. Abosaooda, M., et al.: Role of vitamin C in the protection of the gum and implants in the human body: theoretical and experimental studies. *Int J Corrosion Scale Inhibition*. 10(3), 1213–1229 (2021)
71. Rahbaran, M., et al.: Cloning and embryo splitting in mammals: brief history, methods, and achievements. *Stem Cell. Int.*, 2021–11 (2021). <https://doi.org/10.1155/2021/2347506>
72. Majidi, A., Vacareanu, R.: Evaluation of seismic damage to Iraqi educational reinforced concrete building using FEMA P-58 methodology. In: *IOP Conference Series: Earth and Environmental Science*. IOP Publishing (2021)
73. Hussein, A.A., et al.: Analysis of relationship between design and implementation stages within construction projects in Iraq. In: *IOP Conference Series: Earth and Environmental Science*. IOP Publishing (2021)
74. Assi, L.N., et al.: Early properties of concrete with alkali-activated fly ash as partial cement replacement. In: *Proceedings of the Institution of Civil Engineers-Construction Materials*. 174(1), 13–20 (2021). <https://doi.org/10.1680/jcoma.19.00092>
75. Awad, E.S., et al.: Groundwater hydrogeochemical and quality appraisal for agriculture irrigation in greenbelt area, Iraq. *Environments*. 9(4), 43 (2022). <https://doi.org/10.3390/environments9040043>
76. Widjaja, G., et al.: Mesenchymal stromal/stem cells and their exosomes application in the treatment of intervertebral disc disease: a promising frontier. *Int. Immunopharm.* 105, 108537 (2022). <https://doi.org/10.1016/j.intimp.2022.108537>
77. Jalil, A.T., et al.: Viral hepatitis in Dhi-Qar Province: demographics and hematological characteristics of patients. *Int J Pharmaceutical Res.* 12(1), 2081–2087 (2020)
78. Moghadasi, S., et al.: A paradigm shift in cell-free approach: the emerging role of MSCs-derived exosomes in regenerative medicine. *J. Transl. Med.* 19(1), 1–21 (2021). <https://doi.org/10.1186/s12967-021-02980-6>
79. Jalil, A.T., et al.: Hematological and serological parameters for detection of COVID-19. *J. Microbiol. Biotechnol. Food Sci.* 11(4), e4229 (2022). <https://doi.org/10.55251/jmbfs.4229>
80. Marofi, F., et al.: CAR-NK cell in cancer immunotherapy, A promising frontier. *Cancer Sci.* 112(9), 3427–3436 (2021). <https://doi.org/10.1111/cas.14993>
81. Rudiansyah, M., et al.: Beneficial alterations in growth performance, blood biochemicals, immune responses, and antioxidant capacity of common carp (*Cyprinus carpio*) fed a blend of *Thymus vulgaris*, *Origanum majorana*, and *Satureja hortensis* extracts. *Aquaculture*. 555, 738254 (2022). <https://doi.org/10.1016/j.aquaculture.2022.738254>
82. Elveny, M., et al.: CFD-based simulation to reduce greenhouse gas emissions from industrial plants. *Int. J. Chem. React. Eng.* 19(11), 1179–1186 (2021). <https://doi.org/10.1515/ijcre-2021-0063>
83. Hanan, Z.K., et al.: Detection of human genetic variation in VAC14 gene by ARMA-PCR technique and relation with typhoid fever infection in patients with gallbladder diseases in Thi-Qar province/Iraq. *Mater. Today Proc.* (2021). <https://doi.org/10.1016/j.matpr.2021.05.236>
84. Sadeghi, H., et al.: Iron oxyhydroxide nanoparticles: green synthesis and their cytotoxicity activity against A549 human lung adenocarcinoma cells. *Rendiconti Lincei. Sci. Fis. Nat.* 33(2), 461–469 (2022). <https://doi.org/10.1007/s12210-022-01065-w>
85. Mythili, R., et al.: Utilization of market vegetable waste for silver nanoparticle synthesis and its antibacterial activity. *Mater. Lett.* 225, 101–104 (2018). <https://doi.org/10.1016/j.matlet.2018.04.111>
86. Mythili, R., et al.: Biogenic synthesis, characterization and antibacterial activity of gold nanoparticles synthesised from vegetable waste. *J. Mol. Liq.* 262, 318–321 (2018). <https://doi.org/10.1016/j.molliq.2018.04.087>
87. Chupradit, S., et al.: Use of organic and copper-based nanoparticles on the turbulator installment in a shell tube heat exchanger: a CFD-based simulation approach by using nanofluids. *J. Nanomater.*, 2021–7 (2021). <https://doi.org/10.1155/2021/3250058>
88. Sadeghi, M., et al.: Dichlorosilane adsorption on the Al, Ga, and Zn-doped fullerenes. *Monatshefte für Chemie-Chemical Monthly*. 153(5-6), 1–8 (2022). <https://doi.org/10.1007/s00706-022-02926-8>
89. Isacfranklin, M., et al.: Y2O3 nanorods for cytotoxicity evaluation. *Ceram. Int.* 46(12), 20553–20557 (2020). <https://doi.org/10.1016/j.ceramint.2020.05.172>
90. Isacfranklin, M., et al.: Single-phase Cr2O3 nanoparticles for biomedical applications. *Ceram. Int.* 46(12), 19890–19895 (2020). <https://doi.org/10.1016/j.ceramint.2020.05.050>
91. Raya, I., et al.: Role of compositional changes on thermal, magnetic, and mechanical properties of Fe-PC-based amorphous alloys. *Chin. Phys. B* 31(1), 016401 (2022). <https://doi.org/10.1088/1674-1056/ac3655>
92. Hu, X., et al.: The microchannel type effects on water-Fe3O4 nanofluid atomic behavior: molecular dynamics approach. *J. Taiwan Inst. Chem. Eng.* 135, 104396 (2022). <https://doi.org/10.1016/j.jtice.2022.104396>
93. Olegovich Bokov, D., et al.: Ir-decorated gallium nitride nanotubes as a chemical sensor for recognition of mesalamine drug: a DFT study. *Mol. Simulat.* 48(5), 438–447 (2022). <https://doi.org/10.1080/08927022.2021.2025234>
94. Khaki, N., et al.: Sensing of acetaminophen drug using Zn-doped boron nitride nanocubes: a DFT inspection. *Appl. Biochem. Biotechnol.* 194(6), 1–11 (2022). <https://doi.org/10.1007/s12010-022-03830-x>
95. Saleh, R.O., et al.: Application of aluminum nitride nanotubes as a promising nanocarriers for anticancer drug 5-aminosalicylic acid in drug delivery system. *J. Mol. Liq.* 352, 118676 (2022). <https://doi.org/10.1016/j.molliq.2022.118676>
96. Kartika, R., et al.: Ca12O12 nanocluster as highly sensitive material for the detection of hazardous mustard gas: density-functional theory. *Inorg. Chem. Commun.* 137, 109174 (2022). <https://doi.org/10.1016/j.inoche.2021.109174>
97. Isacfranklin, M., et al.: Synthesis of highly active biocompatible ZrO2 nanorods using a bioextract. *Ceram. Int.* 46(16 Part A), 25915–25920 (2020). <https://doi.org/10.1016/j.ceramint.2020.07.076>
98. Vidhya, M.S., et al.: Anti-cancer applications of Zr, Co, Ni-doped ZnO thin nanoplates. *Mater. Lett.* 283, 128760 (2021). <https://doi.org/10.1016/j.matlet.2020.128760>
99. Turki Jalil, A., et al.: CuO/ZrO2 nanocomposites: facile synthesis, characterization and photocatalytic degradation of tetracycline antibiotic. *J Nanostructures*. 11(2), 333–346 (2021)
100. Jasim, S.A., et al.: Investigation of crotonaldehyde adsorption on pure and Pd-decorated GaN nanotubes: a density functional theory study. *Solid State Commun.* 348-349, 114741 (2022). <https://doi.org/10.1016/j.ssc.2022.114741>
101. Jasim, S.A., et al.: Nanomagnetic Salamo-based-Pd (0) Complex: an efficient heterogeneous catalyst for Suzuki–Miyaura and Heck cross-coupling reactions in aqueous medium. *J. Mol. Struct.* 1261, 132930 (2022). <https://doi.org/10.1016/j.molstruc.2022.132930>
102. Al-Enazi, N.M., et al.: Tin Oxide Nanoparticles (SnO2-NPs) Synthesis Using *Galaxaura Elongata* and its Anti-microbial and Cytotoxicity Study: A Greenery Approach, pp. 1–9. *Applied Nanoscience* (2021)
103. Obaid, R.F., et al.: Antibacterial activity, anti-adherence and antibiofilm activities of plants extracts against *Aggregatibacter actinomycetemcomitans*: an in vitro study in Hilla City, Iraq. *Caspian J Env Sci.* 20(2), 367–372 (2022)
104. Ameen, F., et al.: Flavonoid dihydromyricetin-mediated silver nanoparticles as potential nanomedicine for biomedical treatment of infections caused by opportunistic fungal pathogens. *Res. Chem.*

- Intermed. 44(9), 5063–5073 (2018). <https://doi.org/10.1007/s11164-018-3409-x>
105. Rajadurai, U.M., et al.: Assessment of behavioral changes and antitumor effects of silver nanoparticles synthesized using diosgenin in mice model. *J. Drug Deliv. Sci. Technol.* 66, 102766 (2021). <https://doi.org/10.1016/j.jddst.2021.102766>
 106. Jalil, A.T., et al.: Cancer Stages and Demographical Study of HPV16 in Gene L2 Isolated from Cervical Cancer in Dhi-Qar Province, Iraq, pp. 1–7. *Applied Nanoscience* (2021)
 107. Widjaja, G., et al.: Humoral immune mechanisms involved in protective and pathological immunity during COVID-19. *Hum. Immunol.* 82(10), 733–745 (2021). <https://doi.org/10.1016/j.humimm.2021.06.011>
 108. Saleh, M.M., et al.: Evaluation of immunoglobulins, CD4/CD8 T lymphocyte ratio and interleukin-6 in COVID-19 patients. *Turkish J Immunol.* 8(3), 129–134 (2020). <https://doi.org/10.25002/tji.2020.1347>
 109. Jalil, A.T., et al.: Polymerase chain reaction technique for molecular detection of HPV16 infections among women with cervical cancer in Dhi-Qar Province. *Mater. Today Proc.* (2021). <https://doi.org/10.1016/j.matpr.2021.05.211>
 110. Khan, M.U.F., et al.: Serum level estimation of some biomarkers in diabetic and non-diabetic COVID-19 infected patients. *Appl. Nanosci.*, 1–8 (2022). <https://doi.org/10.1007/s13204-021-02167-x>
 111. Xu, Y., et al.: Prediction of COVID-19 manipulation by selective ACE inhibitory compounds of *Potentilla reptant* root: in silico study and ADMET profile. *Arab. J. Chem.* 15(7), 103942 (2022). <https://doi.org/10.1016/j.arabjc.2022.103942>
 112. Feng, Y., et al.: Pan-cancer analysis and experiments with cell lines reveal that the slightly elevated expression of DLGAP5 is involved in clear cell renal cell carcinoma progression. *Life Sci.* 287, 120056 (2021). <https://doi.org/10.1016/j.lfs.2021.120056>
 113. Xu, Q., et al.: Multi-task joint learning model for segmenting and classifying tongue images using a deep neural network. *IEEE J Biomed Health Infor.* 24(9), 2481–2489 (2020). <https://doi.org/10.1109/jbhi.2020.2986376>
 114. Marofi, F., et al.: Novel CAR T therapy is a ray of hope in the treatment of seriously ill AML patients. *Stem Cell Res. Ther.* 12(1), 465 (2021). <https://doi.org/10.1186/s13287-021-02420-8>
 115. Mohammed, A.E., et al.: In-silico predicting as a tool to develop plant-based biomedicines and nanoparticles: lycium shawii metabolites. *Bio-med. Pharmacother.* 150, 113008 (2022). <https://doi.org/10.1016/j.biopha.2022.113008>
 116. Ameen, F., et al.: Fabrication of silver nanoparticles employing the cyanobacterium *Spirulina platensis* and its bactericidal effect against opportunistic nosocomial pathogens of the respiratory tract. *J. Mol. Struct.* 1217, 128392 (2020). <https://doi.org/10.1016/j.molstruc.2020.128392>
 117. Liu, G., et al.: Combined Antimicrobial Effect of Bacteriocins with Other Hurdles of Physicochemic and Microbiome to Prolong Shelf Life of Food: A Review. *Science of the Total Environment* (2022).154058
 118. Rahman, A., et al.: Identification of potential indigenous microbe from local fermented vegetables with antimicrobial activity. *Galeri Warisan Sains.* 1(1), 01–03 (2017). <https://doi.org/10.26480/gws.01.2017.01.03>
 119. Li, H., Wang, F.: Core-shell chitosan microsphere with antimicrobial and vascularized functions for promoting skin wound healing. *Mater. Des.* 204, 109683 (2021). <https://doi.org/10.1016/j.matdes.2021.109683>
 120. Hamidian, K., et al.: Cytotoxic performance of green synthesized Ag and Mg dual doped ZnO NPs using *Salvadora persica* extract against MDA-MB-231 and MCF-10 cells. *Arab. J. Chem.* 15(5), 103792 (2022). <https://doi.org/10.1016/j.arabjc.2022.103792>
 121. Khatami, M., et al.: Waste-grass-mediated green synthesis of silver nanoparticles and evaluation of their anticancer, antifungal and antibacterial activity. *Green Chem. Lett. Rev.* 11(2), 125–134 (2018). <https://doi.org/10.1080/17518253.2018.1444797>
 122. Haghghat, M., et al.: Cytotoxicity properties of plant-mediated synthesized K-doped ZnO nanostructures. *Bioproc. Biosyst. Eng.* 45(1), 97–105 (2021). <https://doi.org/10.1007/s00449-021-02643-2>
 123. Kumar, V., et al.: Photo-mediated optimized synthesis of silver nanoparticles for the selective detection of Iron(III), antibacterial and antioxidant activity. *Mater. Sci. Eng. C* 71, 1004–1019 (2017). <https://doi.org/10.1016/j.msec.2016.11.013>
 124. Kumar, V., et al.: Size-dependent synthesis of gold nanoparticles and their peroxidase-like activity for the colorimetric detection of glutathione from human blood serum. *ACS Sustain. Chem. Eng.* 6(6), 7662–7675 (2018). <https://doi.org/10.1021/acssuschemeng.8b00503>
 125. Kumar, V., et al.: Photo-induced biosynthesis of silver nanoparticles using aqueous extract of *Erigeron bonariensis* and its catalytic activity against Acridine Orange. *J. Photochem. Photobiol. B Biol.* 155, 39–50 (2016). <https://doi.org/10.1016/j.jphotobiol.2015.12.011>
 126. Kumar, V., et al.: Green synthesis of silver nanoparticle for the selective and sensitive colorimetric detection of mercury (II) ion. *J. Photochem. Photobiol. B Biol.* 168, 67–77 (2017). <https://doi.org/10.1016/j.jphotobiol.2017.01.022>
 127. Kumar, V., et al.: Sunlight-induced green synthesis of silver nanoparticles using aqueous leaf extract of *Polyalthia longifolia* and its antioxidant activity. *Mater. Lett.* 181, 371–377 (2016). <https://doi.org/10.1016/j.matlet.2016.05.097>
 128. Kumar, V., et al.: Photo-induced rapid biosynthesis of silver nanoparticle using aqueous extract of *Xanthium strumarium* and its antibacterial and antileishmanial activity. *J. Ind. Eng. Chem.* 37, 224–236 (2016). <https://doi.org/10.1016/j.jiec.2016.03.032>
 129. Kumar, V., et al.: Photoinduced green synthesis of silver nanoparticles with highly effective antibacterial and hydrogen peroxide sensing properties. *J. Photochem. Photobiol. B Biol.* 162, 374–385 (2016). <https://doi.org/10.1016/j.jphotobiol.2016.06.037>
 130. Kumar, V., et al.: Photoinduced green synthesis of silver nanoparticles using aqueous extract of *Physalis angulata* and its antibacterial and antioxidant activity. *J. Environ. Chem. Eng.* 5(1), 744–756 (2017). <https://doi.org/10.1016/j.jece.2016.12.055>

How to cite this article: Alhomaiddi, E., et al.: Biosynthesis of silver nanoparticles using *Lawsonia inermis* and their biomedical application. *IET Nanobiotechnol.* 16(7-8), 284–294 (2022). <https://doi.org/10.1049/nbt2.12096>